Technical Note GKSS/WMS/01/08
internal report

Numerical Aspects of the Path-Dependence of the *J*-Integral in Incremental Plasticity

How to calculate reliable *J*-values in FE analyses

W. Brocks and I. Scheider

October 2001

Institut für Werkstofforschung
GKSS-Forschungszentrum Geesthacht

1. Introduction

Theories, concepts, and methods which have once been familiar to a few experts, only, can become state of the art and "common" knowledge after some decades. Unfortunately, some of the experts' background information how to apply the respective concepts may get lost during this process, so that people deal with them without realising the underlying assumptions and restrictions. Some examples indicated that such a fate has caught up the *J*-integral which is widely used in rate-independent quasi-static fracture analysis to characterise the energy release rate associated with crack growth. Introduced by CHEREPANOV [1] and RICE [2] in 1967 and 1968, respectively, it found worldwide interest and applications in the 70s, and with increasing capabilities of computers and finite element methods, *J*-based elastic-plastic fracture mechanics became also an issue of numerical computations [3 - 5]. The first calculational round robins starting in 1976 and 1980 by ASTM and ESIS, respectively, exhibited desastrous scatter of the results [3, 4]. The efforts continued [5] and ended in some "Recommendations for use of FEM in fracture mechancis" [6] in 1991. Whereas in the beginning the users were left to there own codes, which gave rise to additional uncertainties and errors, all major commercial FE codes allow for *J* computations. Thus, numerical calculations of *J* for a cracked specimen or structure in elasto-plasticity is now state of the art - provided that some care is taken and some information on the theoretical background of *J* is present. How reliable values of *J* are calculated is the subject and the aim of the present contribution. Whereas standards prescribe how to determine *J* experimentally [7] nothing like this exists for numerical analyses, and the ESIS "recommendations" [6] never reached the level of a document.

2. Theoretical background of the *J*-integral

2.1 Path-independent integrals

Path-independent integrals are used in physics to calculate the intensity of a singularity of a field quantity without knowing the exact shape of this field in the vicinity of the singularity. They are derived from conservation laws.

Let $\varphi(\mathbf{x})$ be a continously differentiable (scalar, vectorial or tensorial) field quantity in the domain $\mathcal{B}$ having the property of

$$\varphi_{,i} := \frac{\partial \varphi}{\partial x_i} = 0 \quad \text{in } \mathcal{B} . \tag{1}$$

Then the GAUSSian divergence theorem states that

$$\int_{\mathcal{B}} \varphi_{,i} \, \mathrm{d}V = \int_{\partial \mathcal{B}} \varphi \, n_i \, \mathrm{d}S = 0 . \tag{2}$$

If a point singularity exists in $\mathcal{B}$, then $\varphi(\mathbf{x})$ is not differentiable in this point and the divergence theorem is only applicable on a domain, $\mathcal{B}_0 = \mathcal{B} - \mathcal{B}_S$, excluding this singularity. The border of $\mathcal{B}_0$ is

$$\partial \mathcal{B}_0 = \partial \mathcal{B} \cup \partial \mathcal{B}_S \cup \partial \mathcal{B}^+ \cup \partial \mathcal{B}^- , \tag{3}$$

see Fig. 1.

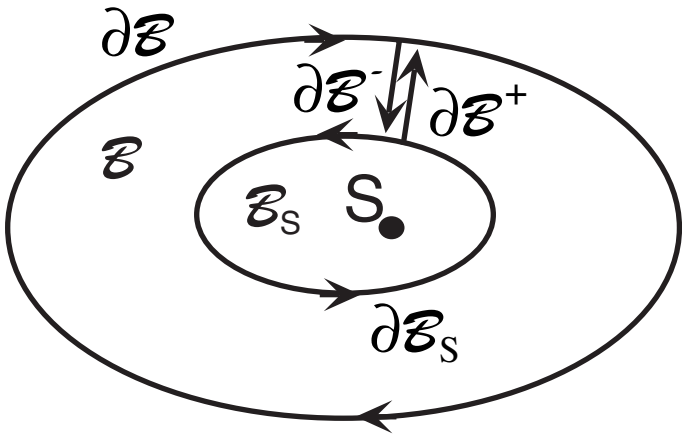

Figure 1: Domain $\mathcal{B}$ containing a singularity S; definition of the border $\partial \mathcal{B}_0$

Then for a closed contour along the border of $\mathcal{B}_0$ we have

$$\oint_{\partial \mathcal{B}_0} \varphi \, n_i \, \mathrm{d}a = \oint_{\partial \mathcal{B}}^{\rightarrow} \varphi \, n_i \, \mathrm{d}S + \int_{\partial \mathcal{B}^+} \varphi \, n_i \, \mathrm{d}S + \oint_{\partial \mathcal{B}_S}^{\leftarrow} \varphi \, n_i \, \mathrm{d}S + \int_{\partial \mathcal{B}^+} \varphi \, n_i \, \mathrm{d}S = 0 . \tag{4}$$

Because of $\int_{\partial\mathcal{E}^+} .. = -\int_{\partial\mathcal{E}^-} ..$ and $\oint^{\rightarrow}_{\partial\mathcal{E}} .. = -\oint^{\leftarrow}_{\partial\mathcal{E}} ..$,

we can conclude the path independence of any contour integral surrounding the singularity in the same sense

$$\oint^{\rightarrow}_{\partial\mathcal{E}} \varphi n_i \,\mathrm{d}S = \oint^{\rightarrow}_{\partial\mathcal{E}_S} \varphi n_i \,\mathrm{d}S\,. \tag{5}$$

Applying a theorem of NOETHER [8], ESHELBY [9] derived a conservation law for the energy momentum tensor

$$P_{ij} = W\delta_{ij} - \frac{\partial W}{\partial u_{k,j}} u_{k,i} \quad \text{with} \quad P_{ij,j} = 0\,. \tag{6}$$

This tensor allows to calculate the material forces acting on defects like dislocations or inclusions

$$F_i = \oint_{\partial\mathcal{E}} P_{ij} n_j \,\mathrm{d}S\,. \tag{7}$$

W can be the strain energy density for a hyper-elastic material, for which

$$\sigma_{ij} = \frac{\partial W}{\partial \varepsilon_{ij}}\,. \tag{8}$$

Other path-independent integrals have been derived by GÜNTHER [10], see also KNOWLES and STERNBERG [11], BUDIANSKY and RICE [12], BUGGISCH et al. [13], KIENZLER [14].

2.2 The *J*-integral

CHEREPANOV [1] and RICE [2] were the first who introduced path-independent integrals into fracture mechanics. RICE [2, 12] also showed that this "*J*-integral" is identical with the energy release rate

$$J = \mathcal{G} = -\left(\partial U/\partial A\right). \tag{9}$$

for a plane crack extension, ΔA. Finally, HUTCHINSON [15], RICE and ROSENGREEN [16] derived the singular stress and strain fields at a crack tip in a power law hardening material, the since called HRR-field, where J plays the role of an intensity factor like K in the case of linear elastic material behaviour. For linear elastic material, J is related to the stress intensity factors by

$$J = \mathcal{G}_{\mathrm{I}} + \mathcal{G}_{\mathrm{II}} + \mathcal{G}_{\mathrm{III}} = \frac{1}{E©}\left(K_{\mathrm{I}}^2 + K_{\mathrm{II}}^2\right) + \frac{1}{2G} K_{\mathrm{III}}^2\,, \tag{10}$$

where I, II, III denote the three fracture modes.

The *J*-integral of elasto-statics can be deduced from the equations governing the static boundary value problem:

equilibrium conditions	$\sigma_{\mathrm{ij,j}} = 0$	in $\mathcal{B}$	(11a)
boundary conditions	$\sigma_{ij} n_i = \bar{t}_j$	on $\partial\mathcal{B}_\sigma$	(11b)
	$u_i = \bar{u}_i$	on $\partial\mathcal{B}_u$	(11c)
small (linear) strain	$\varepsilon_{ij} = \frac{1}{2}\left(u_{i,j} + u_{j,i}\right)$	in $\mathcal{B}$	(11d)
hyperelastic material	$\sigma_{ij} = \dfrac{\partial W}{\partial \varepsilon_{ij}}$	in $\mathcal{B}$	(11e)

We obtain the components of the material force of eq. (7),

$$F_i = \oint_{\partial\mathcal{B}} \left[W(\varepsilon_{mn}) n_i - \sigma_{jk} n_k u_{j,i} \right] \mathrm{d}S, \tag{12}$$

which are non-zero if $\mathcal{B}$ contains a singularity and vanish if not. We apply this integral to a material sheet of constant thickness, h, i.e. $\mathrm{d}S = h\,\mathrm{d}s$, having a straight crack along the x_1-axis, see Fig. 2:

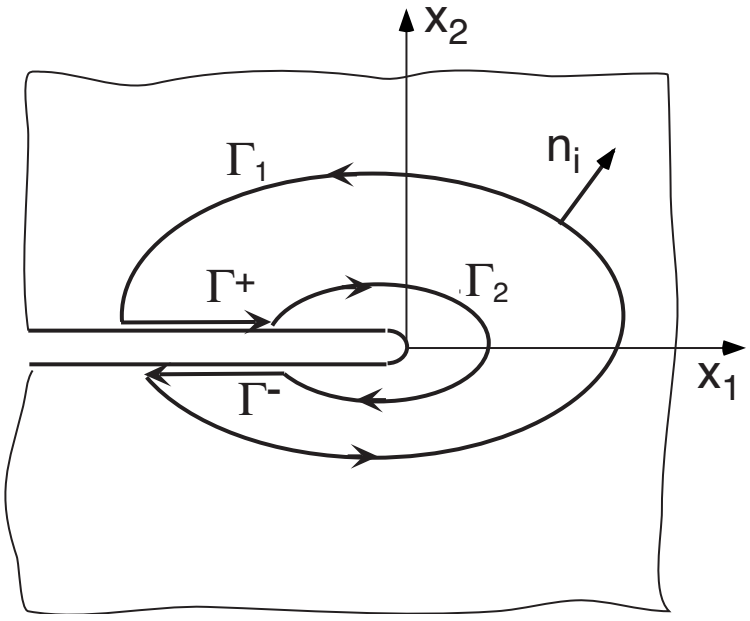

$u_i = u_i(x_1, x_2)$

$\sigma_{ij} = \sigma_{ij}(x_1, x_2)$

$\mathrm{d}S = h\,\mathrm{d}s$

$\mathbf{n} = n_i\,\mathbf{e}_i = \sin\vartheta\,\mathbf{e}_1 + \cos\vartheta\,\mathbf{e}_2$

$\mathrm{d}x_1 = \cos\vartheta\,\mathrm{d}s$

$\mathrm{d}x_2 = \sin\vartheta\,\mathrm{d}s$

Figure 2: Definition of contours for *J*-integral evaluation

The closed contour

$$\Gamma_0 = \Gamma_1 \cup \Gamma^+ \cup \Gamma_2 \cup \Gamma^-, \tag{13}$$

does not include a singularity, and hence

$$\frac{F_i}{h} = \oint_{\Gamma} \left[W n_i - \sigma_{jk} n_k u_{j,i} \right] \mathrm{d}s = \oint_{\Gamma_1}^{\leftarrow} [\ ]\,\mathrm{d}s + \int_{\Gamma^+} [\ ]\,\mathrm{d}s + \oint_{\Gamma_2}^{\rightarrow} [\ ]\,\mathrm{d}s + \int_{\Gamma^-} [\ ]\,\mathrm{d}s = 0 \tag{14}$$

Assuming that the crack borders are straight and stress-free

$$n_i\,\mathrm{d}s = \sin\vartheta\,\mathrm{d}s = \mathrm{d}x_2 = 0 \quad \text{on} \quad \Gamma^+, \Gamma^-, \tag{15a}$$

and

$$\sigma_{jk}\, n_k = \bar{t}_j = 0 \quad \text{on} \quad \Gamma^+, \Gamma^-, \tag{15b}$$

the first components of the integrals along the respective contours, Γ^+, Γ^-, vanish,

$$\int_{\Gamma^+} \left[W\,\mathrm{d}x_2 - \sigma_{jk} n_k u_{j,1}\,\mathrm{d}s \right] = \int_{\Gamma^-} \left[W\,\mathrm{d}x_2 - \sigma_{jk} n_k u_{j,1}\,\mathrm{d}s \right] = 0\ , \tag{16}$$

and because of $\displaystyle\oint_{\Gamma_2}^{\rightarrow} [\ ]\,\mathrm{d}s = -\oint_{\Gamma_2}^{\leftarrow} [\ ]\,\mathrm{d}s$,

we obtain the path independence of the first component of the "*J*-vector"

$$J_1 = \oint_{\Gamma_1}^{\leftarrow} \left[W\,\mathrm{d}x_2 - \sigma_{jk} n_k u_{j,1}\,\mathrm{d}s \right] = \oint_{\Gamma_2}^{\leftarrow} [\ ] = \oint_{\Gamma}^{\leftarrow} [\ ]\ . \tag{17}$$

This holds for the other two components, J_2, J_3, if and only if the contours around the crack tip and the loading are symmetric to the x_1-axis.

This first component of the *J*-vector is the "*J*-integral" as introduced by RICE and CHEREPANOV into fracture mechanics, defining that the integration contour runs anti-clockwise, i.e. mathematically positive, around the crack tip,

$$\boxed{J = \oint_{\Gamma} \left[W\,\mathrm{d}x_2 - \sigma_{jk} n_k u_{j,1}\,\mathrm{d}s \right]}\ . \tag{18}$$

Because of its path independence, it can be calculated in the remote field and characterizes also the near tip situation.

Note, that the following assumptions have been made

(1) time independent processes, no body forces, eq. (11a),

(2) small strains, eq. (11d),

(3) homogeneous hyper-elastic material, eq. (11e),

(4) plane stress and displacement fields, i.e. no dependence on x_3, Fig. 2,

(5) straight and stress-free crack borders parallel to x_1, eq. (15a, b).

2.3 The domain integral or vce method

Calculating a contour integral like eq. (18) is quite unfavourable in finite element codes as coordinates and displacements refer to nodal points and stresses and strains to GAUSSian integration points. Stress fields are generally discontinuous over element boundaries and extrapolation of stresses to nodes requires additional assumptions. Hence, a domain integral method is commonly used to evaluate contour integrals, see e.g. ABAQUS [17].

Applying the divergence theorem again, eq. (2), the contour integral can be re-formulated as an area integral in two dimensions or a volume integral in three dimensions, over a finite domain surrounding the crack front. The method is quite robust in the sense that accurate values are obtained even with quite coarse meshes; because the integral is taken over a domain of elements, so that errors in local solution parameters have less effect. This method was first suggested by PARKS [18, 19] and further worked out by DELORENZI [20].

The J-integral is defined in terms of the energy release rate, eq. (9), associated with a fictitious small crack advance, Δa, see Fig 4,

$$J = \frac{1}{\Delta A_c} \iint_{\mathcal{B}_0} \left[\sigma_{ij} u_{j,k} - W \delta_{ik} \right] \Delta x_{k,i} \, \mathrm{d}S \,, \tag{19}$$

where Δx_k is the shift of the crack front coordinates, ΔA_c the correspondent increase in crack area and the integration domain is the grey area in Fig. 4. Because of this physical interpretation, the domain integral method is also known as "*virtual crack extension*" (vce) method.

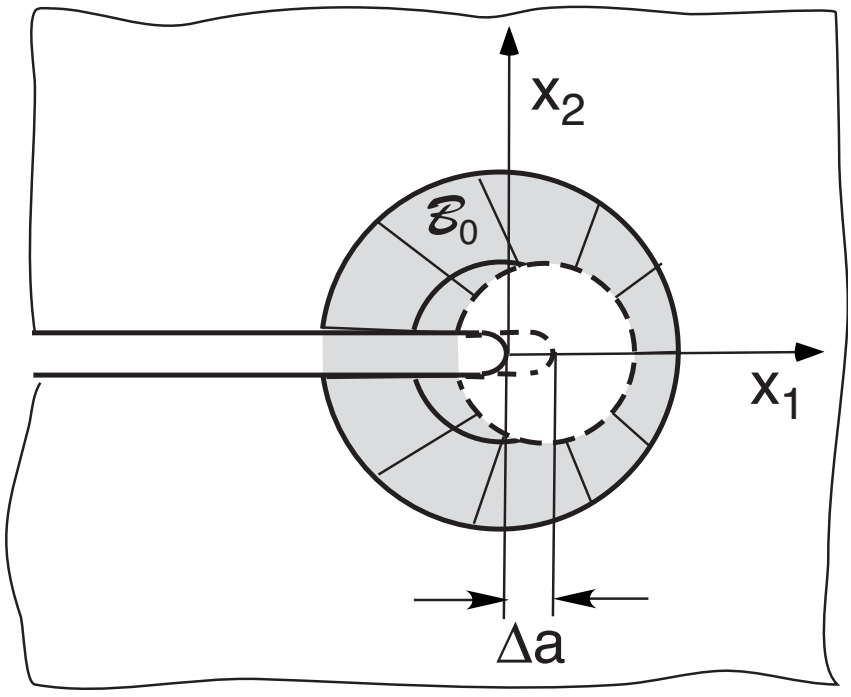

Figure 3: Virtual crack extension

Eq. (19) allows for an arbitrary shift of the crack front coordinates, Δx_k, yielding the energy release rate, $\mathcal{G}_\varphi$, in the respective direction, which can be applied for investigations of mixed mode fracture fracture problems [21]. The common *J*-integral, i.e. the first component of the *J*-vector, $J_1 = \mathcal{G}_\varphi\big|_{\varphi=0}$, is obtained if and only if Δx_k has the direction of x_1 (or ξ_1 in three-dimensional cases, see Fig. 4), which means that it has to be both, perpendicular to the crack plane normal, x_2, and (in three-dimensional cases) the crack front tangent, ξ_3, see section 3.3. In a case where the crack front intersects the external surface of a three-dimensional solid, the virtual crack extension must lie in the plane of the surface. If the vce is chosen perpendicular to the crack plane, i.e. in x_2-direction, one obtains the second component of the *J*-vector, $J_2 = \mathcal{G}_\varphi\big|_{\varphi=\pi/2}$.

For 2-D plane strain or plane stress conditions, the extended crack area is simply $\Delta A_c = t \cdot \Delta a$. In a 3-D analysis, the vce has to be applied to a single node on the crack front if the local value of the energy release rate is sought. For a constant strain element, like the 8-noded 3D isoparametric element, the interpolation functions are linear and a shift of a node on the crack front will result in a triangle, $\Delta A_c = \frac{1}{2}\left(\ell_1 + \ell_2\right) \cdot \Delta a$, where ℓ_1, ℓ_2 are the lengths of the adjacent elements. For the 20-noded isoparametric element, the interpolation functions are of second order, and a node shift will produce a crack area increase of parabolic shape which differs for corner nodes and mid-side nodes. In any case, ΔA_c is linear in Δa and, hence, in $|\Delta x_k|$. Note also, that the crack extension is "virtual" in a sense that it does not change the stress and strain fields at the crack tip.

2.4 Extensions of the *J*-integral

2.4.1 *The three-dimensional J*

Assuming plane crack surfaces, the *J*-integral may be applied to three-dimensional problems. It is defined locally, $J(s_R)$, s_R being the curved crack front coordinate, following the concepts of KIKUCHI et al. [22], AMESTOY et al. [23] and BAKKER [24]. Suppose, the crack is in the (x_1, x_3)-plane, then a local coordinate system (ξ_1, ξ_2=x_2, ξ_3) is introduced in any point P tangential to the crack front, see Fig. 3, so that the (ξ_1, ξ_3)-plane is perpendicular to the crack.

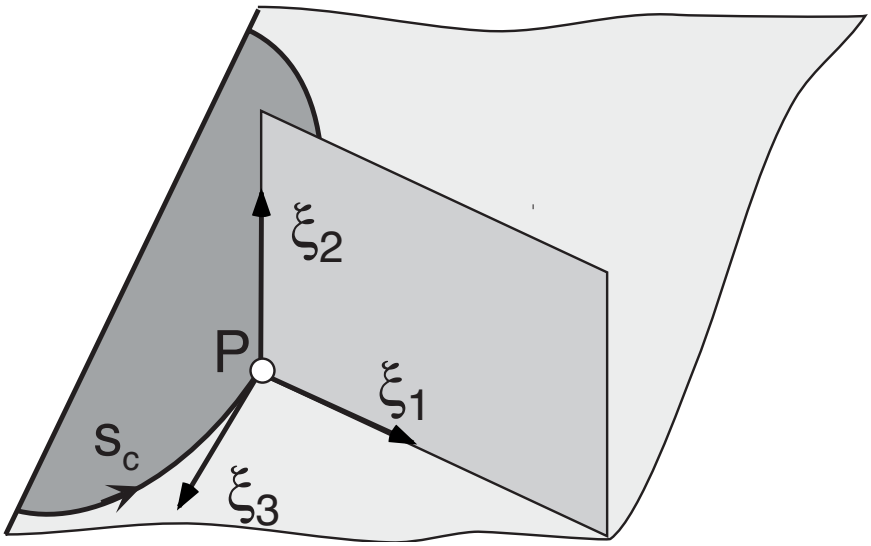

Figure 4: Definition of the local *J*-integral evaluation for three-dimensional problems

The domain, $\mathcal{B}_0 = \mathcal{B} - \mathcal{B}_S$, is again a material sheet of constant thickness, h, with $h \to 0$, but as this is a three-dimensional problem, its border now also contains the upper and lower faces, $\mathcal{S}^+$ and $\mathcal{S}^-$, in the (ξ_1, ξ_2)-plane,

$$\partial\mathcal{B}_0 = \Gamma_1 \cup \Gamma^+ \cup \Gamma_2 \cup \Gamma^- \cup \mathcal{S}^+ \cup \mathcal{S}^- . \tag{21}$$

Eq. (12) becomes

$$F_i = h\left\{ \oint_{\Gamma_1}^{\leftarrow} [\ ]\,\mathrm{d}s + \int_{\Gamma^+} [\ ]\,\mathrm{d}s + \oint_{\Gamma_2}^{\rightarrow} [\ ]\,\mathrm{d}s + \int_{\Gamma^-} [\ ]\,\mathrm{d}s \right\} + \iint_{\mathcal{S}^+} [\ ]\,\mathrm{d}S + \iint_{\mathcal{S}^-} [\ ]\,\mathrm{d}S = 0 , \tag{21}$$

and for an infinitesimal thickness h, the TAYLOR expansion

$$\iint_{\mathcal{S}^+} [\ ]\,\mathrm{d}S + = -\iint_{\mathcal{S}^-} [\ ]\,\mathrm{d}S - h\iint_{\mathcal{S}^-} \frac{\partial [\ ]}{\partial \xi_3}\,\mathrm{d}S \tag{22}$$

holds. With the same assumptions as in eqs. (15a, b) and the same arguments as above, the first component of the three-dimensional *J*-integral is obtained.

$$J(s_c) = \oint_{\Gamma_1}^{\leftarrow} \left[W\,\mathrm{d}x_2 - \sigma_{jk} n_k u_{j,1}\,\mathrm{d}s \right] - \iint_{\mathcal{S}^-} \frac{\partial}{\partial \xi_3} \left[W - \sigma_{jk} n_k u_{j,1} \right] \mathrm{d}S , \tag{23}$$

which is a local value, i.e. it varies along the crack front. The second term vanishes if J is constant with respect to the crack front coordinate; it may contribute significantly if strong gradients occur, e.g. at the specimen surface.

Applying the domain integral method, the volume integral of eq. (19) already includes three-dimensional "effects" [20, 24]. If the whole crack front is shifted by the same amount, Δa, an

average value, $\bar{J} = \frac{1}{\ell_c}\int_0^{\ell_c} J(s_c)\,\mathrm{d}s_c$, for the total structure is obtained as in the experimental procedures [7] where J is evaluated from the area under the load vs displacement curve.

2.4.2 *Body forces, surface tractions and thermal loading*

The fundamental eq. (11a) for deriving the path independence postulates that the stress tensor is divergence free. These equilibrium conditions are restricted to static and stationary processes without body forces or heat sources acting in $\mathcal{B}$. Constant body forces like gravitational forces, which have a potential not explicitly depending on the coordinates, x_i, can easily be included in the W-term and do not affect path independence, see e.g. [14]. In all other cases, J becomes path dependent unless an extra term is added [25, 26]:

$$J = \frac{1}{\Delta A_c}\iiint_V \left[\left(\sigma_{ij}u_{j,k} - W\delta_{ik}\right)\Delta x_{k,i} - f_i u_{i,j}\Delta x_j\right]\mathrm{d}v \ . \tag{24}$$

The forces f_i can be body forces like gravitational forces, $f = \rho g$, or "acceleration forces", $f_i = \rho\ddot{u}_i$, in the case of dynamic loading.

In addition, the boundary conditions, eq. (15a), postulate that the crack faces are Γ^+, Γ^-, are traction free. If this condition is not met, path independence has to be re-established again by a surface correction term,

$$J = \frac{1}{\Delta A_c}\left\{\iiint_V [\ ]\mathrm{d}v - \iint_{\partial V_c} t_i\, u_{i,j}\Delta x_j\,\mathrm{d}S\right\}, \tag{25}$$

where the vector t_i represents the surface tractions (or pressure) acting on the crack faces, ∂V_c, [25, 26].

The correction term for thermal fields is

$$J = \frac{1}{\Delta A_c}\left\{\iiint_V [\ ]\mathrm{d}v + \iiint_V \sigma_{ij}\left[\frac{\partial\alpha}{\partial\Theta}\left(\Theta - \Theta_0\right) + \alpha\right]\frac{\partial\Theta}{\partial x_k}\delta_{ij}\,\Delta x_k\,\mathrm{d}v\right\} \ . \tag{26}$$

where $\Theta(x_i)$ is the temperature field, Θ_0 the reference temperature and α the coefficient of thermal expansion [26, 27].

2.4.3 *Multi-phase materials*

Path independence of J only holds only if the material is homogeneous. However, the assessment of defects in composite or gradient materials or in welded structures requires an extension of J to multi-phase materials. Again, correction terms have to be added to re-establish

path independence. Moreover, the boundary conditions become asymmetric in these cases (mixed mode problem), so that a single component of J is insufficient to characterize the crack field and the complete "J-vector"

$$J_i = \oint_{\Gamma} \left[W n_i - \sigma_{jk} n_k u_{j,i} \right] \mathrm{d}s \tag{27}$$

has to be considered. In a 2-D problem, this reduces to J_1 and J_2 which are related to the stress intensity factors in linear elastic fracture mechanics by

$$J_1 = \frac{1}{E'} \left(K_{\mathrm{I}}^2 + K_{\mathrm{II}}^2 \right) \quad , \quad J_1 = -\frac{2}{E'} K_{\mathrm{I}} K_{\mathrm{II}} . \tag{28}$$

If the contour Γ passes a phase boundary between two materials near the crack tip, it includes an additional singularity of stresses and strains. This contribution has to be eliminated by a closed contour integral along this interface, see [28] and Fig. 5,

$$J_i = \oint_{\Gamma} \left[W n_i - \sigma_{jk} n_k u_{j,i} \right] \mathrm{d}s - \oint_{\Gamma_{\mathrm{pb}}} \left[W n_i - \sigma_{jk} n_k u_{j,i} \right] \mathrm{d}s \ . \tag{29}$$

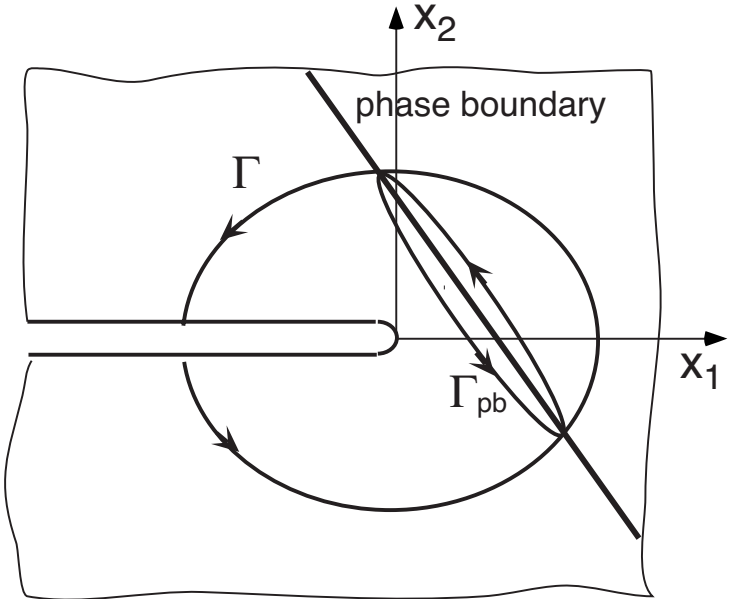

Figure 5: Contours for J-integral evaluation at a crack tip located near a phase boundary

2.5 Path dependence of the J-integral in incremental plasticity

The severest restriction for J results from the assumed existence of a strain energy density, W, as a potential from which stresses can be uniquely derived. This assumption also conceals behind frequently used expressions like "deformation theory of plasticity" [15, 16] or HENCKY's theory of "finite plasticity". But it actually does not describe irreversible plastic deformations as in the "incremental theory of plasticity" of VON MISES, PRANDTL and REUSS, but "hyperelastic" or non-linear elastic behaviour. It does not only exclude any local unloading processes but also any

local re-arranging of stresses, i.e. changing of loading direction in the stress space, resulting from the yield condition. All loading paths in the stress space are supposed to remain "radial" so that the ratios of principal stresses do not change with time. The condition of monotonous global loading of a structure is of course not sufficient to guarantee radial stress paths in non-homogeneous stress fields. Hence, the *J*-integral will become path dependent as soon as plasticity occurs and the contour Γ passes the plastic zone.

For small scale and contained yielding, a path independent integral can be computed outside the plastic zone. This means that Γ - or the respective evaluation domain - has to be large enough to surround the plastic zone and pass through the elastic region only. In gross plasticity, this is not possible, and some more or less pronounced path-dependence will always occur, so that the evaluation of a "path-independent" integral is a question of numerical accuracy. Because of its relation to the global energy release rate, eq. (9), which is used to evaluate *J* from fracture mechanics test results, *J* has to be understood as a "saturated" value reached in the "far-field" remote from the crack tip. Any kind of "near-field" integrals as in [29, 30] are physically meaningless [31]. As *J* is a monotonously increasing function of the distance, *r*, to the crack tip [32, 33] - any other behaviour would mean an "energy production" instead of energy dissipation and hence violate the second law of thermodynamics - the highest calculated *J*-value with increasing domain size is always the closest to the "real" far-field *J*,

$$J_{\text{tip}} \le J(r) \le J_{\text{far field}} \ . \tag{30}$$

Significant stress re-arrangements occur at a blunting crack tip and the path dependence increases strongly. Moreover, *J* will keep a finite value in the limit of a vanishingly small contour if and only if the strain energy density, *W*, has a singularity of the order of r^{-1},

$$J_{\text{tip}} = \lim_{\Gamma \to 0} \oint_{\Gamma} \left[W \, \mathrm{d}x_2 - \sigma_{jk} n_k u_{j,1} \, \mathrm{d}s \right] = \lim_{r \to 0} \int_{-\pi/2}^{+\pi/2} W r \cos\vartheta \, \mathrm{d}\vartheta \ . \tag{31}$$

This holds in linear elasticity where stresses and strains have a $1/\sqrt{r}$-singularity and for HRR-like fields [15, 16]. As the stress singularity at the blunting crack tip vanishes under the assumption of finite strains and incremental plasticity, *J* will not have a finite value any more,

$$J_{\text{tip}} = \lim_{\Gamma \to 0} \oint_{\Gamma} \left[W \, \mathrm{d}x_2 - \sigma_{jk} n_k u_{j,1} \, \mathrm{d}s \right] = 0 \ . \tag{32}$$

The same effect occurs at growing cracks [31-33], where stresses and strains are still singular but their singularity is not strong enough to provide a non-zero local energy release rate, as was addressed long ago by RICE [34, 35] as the "paradox of elastic-plastic fracture mechanics", stating that no "energy surplus" exists for crack propagation.

Examples of path dependence of *J* in incremental plasticity are given in section 4.3.

3. *J*-integral calculation with ABAQUS

3.1 Contour integral evaluation by the domain integral method

The ABAQUS User's Manual [17] states in section 7.8.2: "*Several contour integral evaluations are possible at each location along the crack front. In a finite element model each evaluation can be thought of as the virtual motion of a block of material surrounding the crack tip. Each such block is defined by contours: each contour is a ring of elements completely surrounding the crack tip or crack front from one crack face to the opposite crack face. These rings of elements are defined recursively to surround all previous contours.*"

This is in accordance with Figs. 3 and 4, defining the vce method and the three-dimensional generalization of *J*.

"ABAQUS *automatically finds the elements that form each ring from the node sets given as the crack tip or crack-front definition. Each contour provides an evaluation of the contour integral. The number of evaluations possible is the number of such rings of elements. The user must specify the number of contours to be used in calculating contour integrals by using the* CONTOURS *parameter on the* *CONTOUR INTEGRAL *option.*"

According to what was said in section 2.5 on path dependence, the number of contours should be high enough to check if a saturated far-field value has been reached.

"*The J-integral is defined in terms of the energy release rate associated with crack advance*" (see section 2.3). *For a virtual crack advance of* $\lambda(s)$ *in the plane of a three dimensional fracture* [1], *the energy release rate is given by*

$$J = \int_A \lambda \left[\sigma_{ij} u_{j,k} - W \delta_{ik} \right] n_i \, q_k \, \mathrm{d}A \ .$$

where dA is a surface element along a vanishing small tubular surface enclosing the crack tip; **n** *is the outward normal to dA; and* **q** *is the local direction of virtual crack propagation.*"

See Fig. 3 and compare eq. (19) with apparently $\lambda q_k \triangleq \frac{\Delta x_k}{\Delta A_c}$, $\mathrm{d}A \triangleq \mathrm{d}v$, and $A \triangleq \mathcal{B}_0$ (not to be mixed with the virtual crack extension area, A_c). The actual meaning of **n** does not become clear here; it is specified as "the normal to the crack plane", later, see section 3.3.

"*For elastic material behavior W is elastic strain energy; for elastic-plastic or elasto-viscoplastic material behavior W is defined as the elastic strain energy density plus the plastic dissipation, thus representing the strain energy in an "equivalent elastic material".*

This "*equivalent elastic material*" corresponds to the assumption of "deformation theory of plasticity". *W* is the total area under the uniaxial stress-strain curve,

---

[1] a three-dimensional crack configuration as in Fig. 4 is obviously meant, here.

$$W = W^{\mathrm{e}}_{\mathrm{vol}} + W^{\mathrm{e}}_{\mathrm{shape}} + W^{\mathrm{p}}_{\mathrm{shape}} = \frac{1-2\nu}{6E}\sigma_{kk}^2 + \frac{1+\nu}{3E}\overline{\sigma}^2 + \int_0^t \overline{\sigma}\,\dot{\overline{\varepsilon}}^{p}\,\mathrm{d}\tau \ , \tag{32}$$

where $\overline{\sigma}^2 = \frac{3}{2}\sigma'_{ij}\sigma'_{ij}$ and $\dot{\overline{\varepsilon}}^{p2} = \frac{2}{2}\dot{\varepsilon}^{p}_{ij}\dot{\varepsilon}^{p}_{ij}$ are VON MISES effective stress and plastic strain rate, respectively.

"*Therefore, the J-Integral calculated is suitable only for monotonic loading of elastic-plastic materials*."

This is a potentially misleading statement, as monotonic loading is a necessary but not a sufficient condition for path independence of *J*, see section 2.5.

3.2 Domain dependence

"*The J-integral should be independent of the domain used, but J-integral estimates from different rings may vary because of the approximate nature of the finite element solution; strong variation in these estimates, commonly called domain dependence or contour dependence, indicates a need for mesh refinement (provided that the problem is suitable for contour integrals)*."

This is a fundamental misunderstanding! Path (or domain dependence) is not a result of "*the approximate nature of the finite element solution*" but of the differences which exist between "deformation theory" and "incremental theory" of plasticity, as was outlined in section 2.5. Hence, contour dependence does not at all indicate "*a need for mesh refinement*". As stated above, the domain integral method is quite robust in the sense that accurate values are obtained even with quite coarse meshes, and a far-field *J* has to be evaluated in any case.

"*Numerical tests suggest that the estimate from the first ring of elements abutting the crack front does not provide a high accuracy result, so at least two contours are recommended*."

The first part is absolutely true, but trivial, the given recommendation however is by no means sufficient. Even two contours are not sufficient, in general, see section 4.3. The manual also misses to explain what to do with the two values obtained from two contours!

3.3 Requested input

"*Contour integrals along several different crack tips can be evaluated at any time by repeating the* *CONTOUR INTEGRAL *option as often as needed in the step definition. The user must specify the node set forming each crack tip (or the node sets forming the crack front in three-dimensional solid meshes), the direction of crack propagation at each crack tip, and the number of contours defining groups of elements to be used in separate evaluations of the same contour integral*".

3.3.1 *Defining the crack front*

"*The user must provide a list of all the node sets that define the crack front. For two-dimensional cases only one node set ... must be given. For three-dimensional cases, one node set must be given for each node (or cluster of focused nodes) along the crack front. These sets must be given in order from one end of the crack to the other and must include the midside nodes of second-order elements*."

"*If blunted cracks are modeled, the nodes of the crack front node set should include all of the nodes going from one crack face to the other that would collapse onto the crack tip if the radius of the blunted crack tip were reduced to zero*."

3.3.2 *Defining surface normals*

"*In a case where the crack front intersects the external surface of a three-dimensional solid, where there is a surface of material discontinuity in the model, or where the crack is a curved shell, the virtual crack extension*, **q**, *must lie in the plane of the surface for accurate contour integral evaluation*."

3.3.3 *Specifying the crack propagation direction*

"*The user must specify the direction of virtual crack extension at each crack-tip node set by specifying either the normal to the crack plane*, **n**, *or the crack extension direction*, **q**."

n and **q** correspond to $x_2 = \xi_2$ and ξ_1 in Fig. 4, respectively.

"*If the crack extension direction is specified in the 'straight ahead' or 'self-similar' direction, the contour integral values will be positive, which corresponds to crack growth or energy released. Negative contour values are obtained when the crack extension direction is specified in the opposite direction and correspond to energy needed to obtain crack closure*."

3.3.4 *Specifying the normal direction*

"*The crack extension direction can be defined by specifying the normal,* **n**, *to the crack plane by including the* NORMAL parameter to the *CONTOUR INTEGRAL *option. If the normal is specified,* ABAQUS *will calculate a crack extension direction,* **q**, *that is orthogonal to the crack front tangent,* **t**, *and the normal,* **n**. *... Using the* NORMAL *parameter implies that the crack front is flat*."

3.3.5 *Specifying the crack extension direction*

"*Alternatively, the crack extension direction*, **q**, *can be specified directly by omitting the* NORMAL *parameter. In three dimensions the crack propagation direction,* **q**, *will be corrected to be orthogonal to any normal defined at a node, or in other cases, to the crack front itself. The tangent,* **t**, *to the crack front at a particular point is obtained by parabolic interpolation through the crack front node set for which the propagation vector is defined and the nearest node sets on either side of this node set. The crack front location is defined by the coordinates of the first node in each crack front node set.* ABAQUS *will normalize the crack extension direction,* **q**."

These "automatic" corrections prevent input errors by the user; they inhibit any possibilities of calculating anything else but the J_1 component, however, see remark in section 2.3. As also stated in section 2.3, the results of eq. (19) are independent of the magnitude of virtual crack extension, Δa.

3.3.6 *Symmetry*

"*If the crack front is defined on a symmetry plane, only half of the structure needs to be modeled. The* SYMM *parameter on the* *CONTOUR INTEGRAL *option should be used in this case. The change in potential energy calculated from the virtual crack front advance is doubled to compute the correct contour integral values.*"

3.4 Constructing fracture mechanics meshes for small-strain and finite-strain analyses

"*Sharp cracks (where the crack faces lie on top of one another in the undeformed configuration) are usually modeled using small-strain assumptions. Focused meshes ... should normally be used for small-strain fracture mechanics evaluations. However, for a sharp crack the strain field becomes singular at the crack tip. This result is obviously an approximation to the physics; however, the large-strain zone is very localized, and most fracture mechanics problems can be solved satisfactorily using only small-strain analysis.*"

Several nearly or partly true statements are mixed up here. Singular elements (*focused meshes*) at the crack tip are not necessary if only *J* is to be evaluated. They have been introduced to model the singular strain fields in linear-elastic and elasto-plastic fracture mechanics under small-strain assumption [36]. Singular crack tip elements were necessary for stress intensity factor evaluations as long as these were based on the extrapolation of stress or displacement fields. They are not required if *K*-factors are evaluated from eq. (10) by a *J*-analysis [37].

Now concerning the question of small- or finite-strain analysis: correct *J*-values will be obtained in a small-strain analysis, and problems of path-dependence are much less significant, see

sections 2.5 and 4.3. As "*the large-strain zone is very localized*", indeed, the crack tip meshing and the small-strain assumption will change the crack tip fields, but neither affect the global load-displacement behaviour nor the (far-field) *J*-value.

"*In large-strain analysis ... singular elements should not normally be used. The mesh must be sufficiently refined to model the very high strain gradients around the crack tip if details in these regions are required. Even if only the J-integral is required, the deformation around the crack tip may dominate the solution and the crack-tip region will have to be modeled with sufficient detail to avoid numerical problems*."

Most of this is simply wrong. There exist singular elements which under the assumption of large strains are able to model crack tip blunting [38, 39]. Thus, if local stress and strain fields are to be evaluated, these elements have to be used. If only the *J*-integral is required, neither singular elements nor a large-strain analysis must be applied. "*Numerical problems*" are more likely if a very fine mesh at the crack tip is used [39].

3.5 General options

3.5.1 *Loads*

"*Contour integral calculations include the following distributed load types:*

- *thermal loads;*
- *crack face loads on continuum elements;*
- *uniform body forces;*
- *centrifugal loads on continuum elements*."

See section 2.4.2.

3.5.2 *Material options*

"*J-integral calculations are valid for linear-elastic, nonlinear elastic, and elastic-plastic materials. Plastic behavior can be modeled as nonlinear elastic ("Deformation plasticity"), but the results are generally best if the material is modeled by incremental plasticity and is subject to proportional monotonic traction loading*".

Again, partly true statements are mixed up with wrong ones; in particular, physical arguments are confused with numerical ones. The meaning of "valid" is diffuse: whether or not *J* is a physically meaningful parameter in elastic-plastic fracture mechanics is a still controversial physical question; nevertheless, "correct" values can be calculated in the context of the underlying theory. With respect to theoretical foundation, the "best" results are obtained with deformation plasticity, not with incremental plasticity, of course. However, physical reality of material behaviour is modelled more appropriately with incremental plasticity. The condition of

"*proportional monotonic traction loading*" relates to the fact, that differences between incremental plasticity and deformation plasticity are least in this assumption - that is why the results are "best".

3.5.3 *Elements*

"*The contour integral evaluation capability of* ABAQUS *assumes that the elements that lie within the domain used for the calculations are quadrilaterals in two-dimensional or shell models or bricks in continuum three-dimensional models. Triangles, tetrahedra, or wedges should not be used in the mesh that is included in the contour integral regions*".

Any indication what might go wrong with triangles, tetrahedra, or wedges is unfortunately missing in this statement.

4. Numerical Example

4.1 Specimen and FE model

The specimen used for determination of the *J*-integral is a so-called compact tension, C(T), specimen of width W = 50 mm, shown in Fig. 6, which is a standard specimen for the determination of the fracture resistance of materials, e.g. [7].

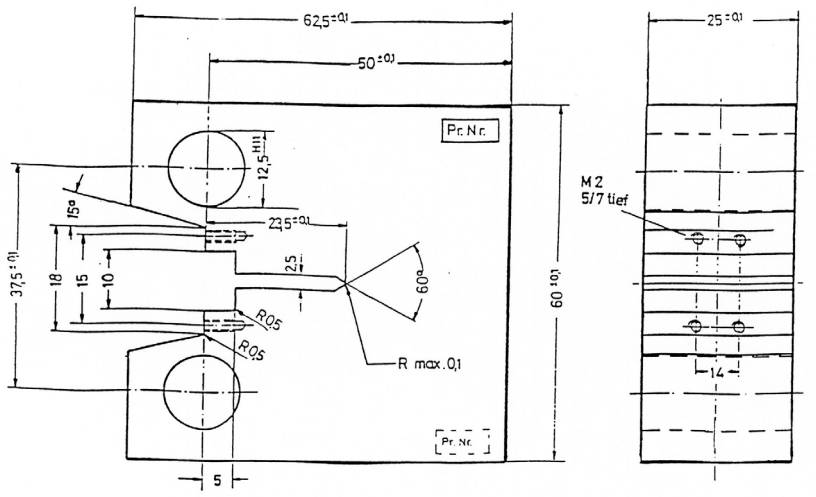

Figure 6: Technical drawing of the C(T) specimen

The finite element model of the specimen is two-dimensional assuming plane strain conditions. Due to symmetry, only one half of the specimen needs to be modelled; symmetry is established by boundary conditions, namely zero desplacements in *y*-direction, applied to the nodes in the ligament. The mesh, consisting of 376 eight-noded ("quadratic") elements, is shown in Fig. 7. Loading is realized by a prescribed displacement of the node in the center of the pin hole which is connected to the specimen by a quarter circle of elastic elements; the corresponding reaction force is calculated by the FE programme. The load line displacement, V_{LL}, is evaluated at the point below the load point, indicated by a diamond in Fig. 7.

The mesh around the crack tip is refined, the element length being 50 μm, as shown in Fig. 8. This mesh, which has been proposed for an ESIS numerical round robin on cleavage fracture predictions, is not typical for ductile fracture analyses, see e.g. [6], but it will be shown in section 4.3 that the *J*-integral results have a sufficient accuracy. However, the stress singularity at the crack tip cannot be described correctly with this kind of mesh.

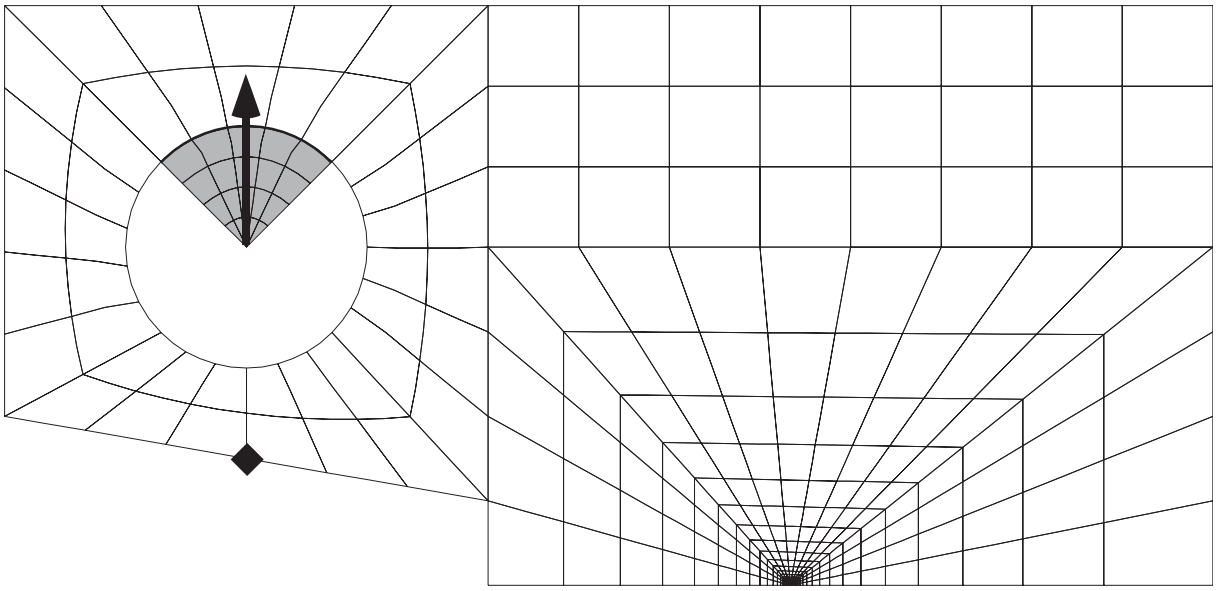

Figure 7: Finite element mesh for the C(T) specimen; the point where the load line displacement, V_{LL}, is evaluated is marked by the diamond.

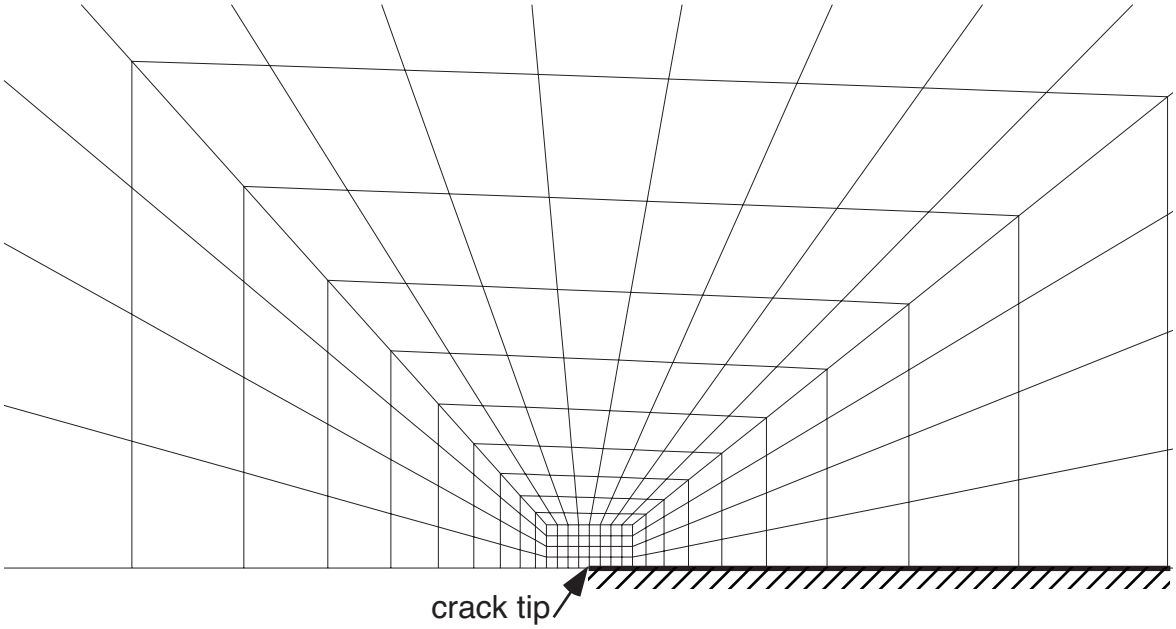

Figure 8: Detail of the finite element mesh showing the elements around the crack tip.

The material curve used for the calculations is that of a low alloy ferritic steel (German designation 22 Ni Mo Cr 3 7). The true stress vs logarithmic strain curve is shown in Fig. 9. The elastic properties are E = 213 GPa and ν=0.3.

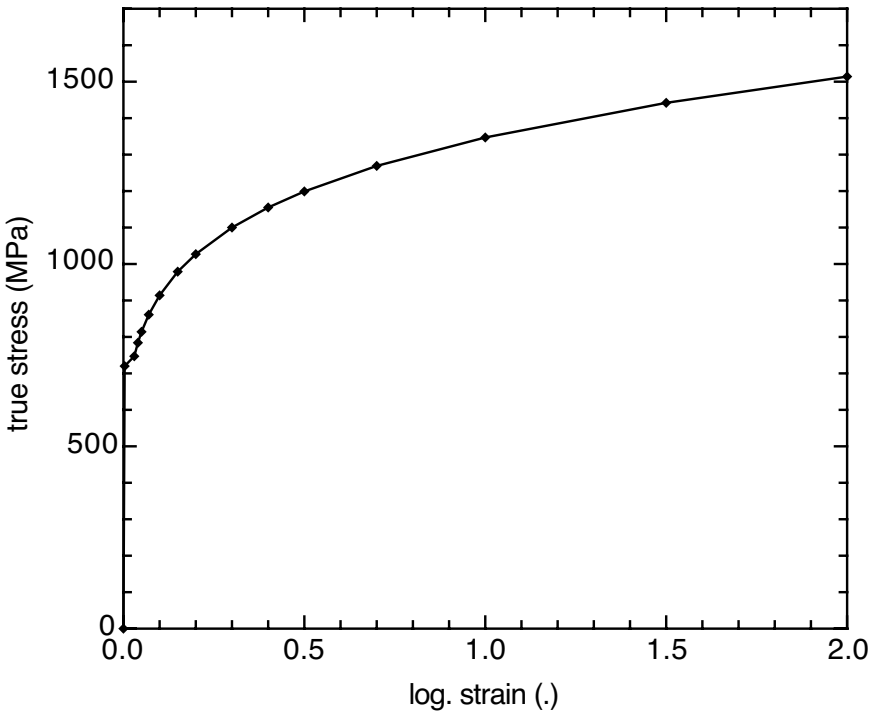

Figure 9: True stress – logarithmic strain curve for 22 Ni Mo Cr 3 7.

4.2 Input data and contours for *J*-calculation

4.2.1 *Input data for the J evaluation*

As already explained in section 3.3, the command *CONTOUR INTEGRAL is used for the *J*-integral evaluation. For doing this, a node set has to be defined which contains the crack tip node(s):

```
**
** CRACK TIP NODE SET
**
*NSET, NSET=CRACKTIP
 1,
**
```

In the present example, the crack tip node has the number 1. If the crack tip is modelled by multiple nodes due to a discretization using collapsed elements, all of these nodes have to be defined in the node set. The name of the node set, here: CRACKTIP, can be chosen by the user. An important information is missing in the ABAQUS manual: It is not necessary that just the crack tip node(s) are defined in this node set. The node set can contain an arbitrary number of nodes, which meet the following restrictions:

1) they contain the crack tip node itself;

2) they form a closed domain,

3) they may not lie on the boundary of the structure.

If a node set is defined which contains more than the crack tip node, ABAQUS will give a warning message to the output file (.dat) for each node, which has not the same position as the first node of that node set:

```
***WARNING: THE COORDINATES OF NODES WITHIN THE SAME CLUSTER ARE NOT
            IDENTICAL. THIS IS THE CASE FOR NODES XXX YYY
```

where XXX is the number of the first node in the node set (assuming that this is the crack tip node). The user can ignore the message as long as he considers the restrictions mentioned above. The advantage of defining a larger region for the contour integral is that the user has a more effective control on the contour region taken by ABAQUS. It is recommended to define a large region around the crack tip by the node set and only a few contours around this set by the CONTOURS parameter, instead of defining only the crack tip node and many contours around the node. However, in the mesh used for the example only the crack tip node has been used to explain the generation of contours around it. The first nine contours around the crack tip are shown in Fig. 10. The contours include the respective virtually shifted domains, see Fig. 3, and stress and strain contributions to the *J*-integral result from the ring of elements outside the respective contour.

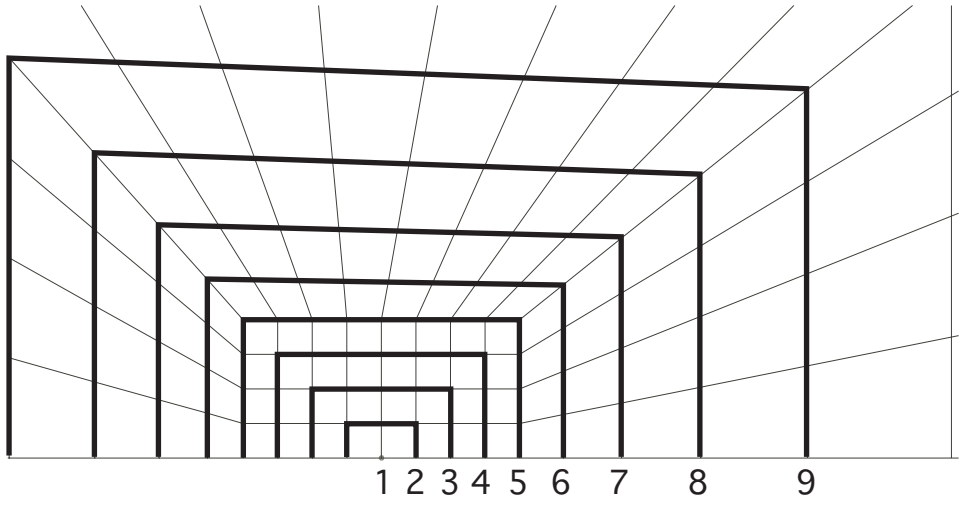

Figure 10:

It is important to note that the contour 21 reaches the outer border of the specimen. In this case, no complete ring of elements exists outside the shifted domain (defined by the respective node set), which leads to wrong values for the *J*-integral, as will be shown in section 4.3.

The request for the contour integral calculation is done by the command *CONTOUR INTEGRAL:

```
**
** J-INTEGRAL DEFINITION
**
*CONTOUR INTEGRAL, CONTOURS=21, SYMM, OUTPUT=BOTH
 CRACKTIP, 1.0, 0.0
**
```

Here, the definition of crack propagation direction is given by the crack extension direction, **q**, see section 3.3. In a two-dimensional calculation, the declaration of two components of the vector is sufficient. The OUTPUT parameter defines where the *J* values will be recorded; OUTPUT=FILE causes the results to be written in the results (.fil) file. If OUTPUT=BOTH is set, the results will be written to the results and the data (.dat) file. If the results shall only be written to the data file, the parameter can be omitted.

It is also be possible to define the contour integral using the crack tip normal. In this case the command is:

```
**
** J-INTEGRAL DEFINITION
**
*CONTOUR INTEGRAL, CONTOURS=21, SYMM, NORMAL, OUTPUT=BOTH
 CRACKTIP, 0.0, 1.0
**
```

4.2.2 *Problems caused by the definition of many contours*

The problem caused by the definition of a single crack tip node can be illustrated in a different mesh, which is shown in Fig. 11. In this mesh the elements around the ligament are small whereas the element size in other regions increases quite fast, which is a common mesh design for crack propagation analyses. If one defines only the crack tip node in this case, even a large number of contours may not guarantee a sufficiently close approach to the far field *J*-integral value. For this mesh a node set containing all nodes in the grey region would lead to much better results. A few contours are enough to control the path independence of the *J*-integral.

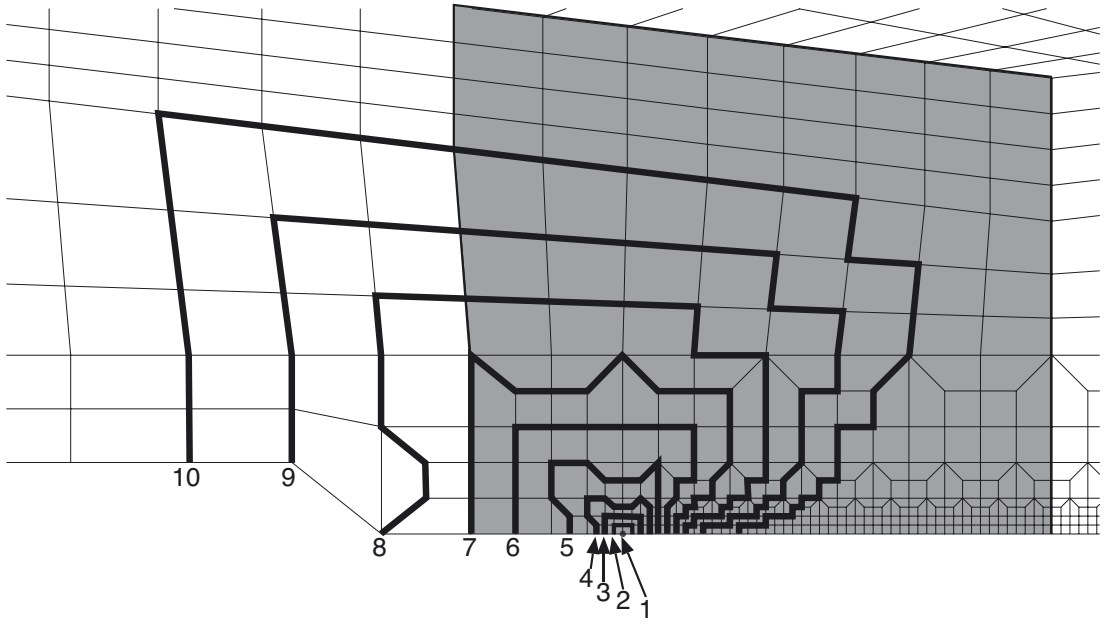

Figure 11: Contours paths generated by ABAQUS when a single crack tip node is defined in a mesh used for crack propagation analysis; the grey shaded region is an alternative for the definition of a cluster of nodes, which leads to better results of the *J*-integral calculation.

It should be noted that the meshes typically used for fracture analyses do not lead to such problems, since the elements are arranged in a radial manner, as shown in Fig.12 for a blunted crack tip. However, also in those meshes it is a better practice to define a whole domain as crack-tip node set, since the number of contours necessary for reaching the far field value of the *J*-integral can be considerably high. In addition, the contours generated by ABAQUS extend by the same number of elements in the direction of the stress free crack surface as in the ligament direction, see Figs. 11 and 12, which is not very efficient for the analysis as the main contributions to *J* result from the highly plastified areas along the ligament.

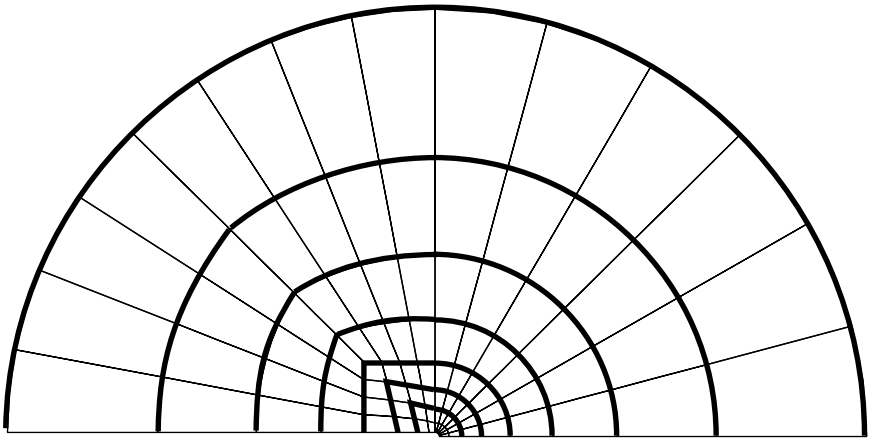

Figure 12: Mesh detail with a blunted crack tip typically used for an elastic-plastic fracture analysis. The thick lines indicate nine contours automatically generated by ABAQUS when the cluster of nodes at the crack tip is defined by the user.

4.2.3 *Definition of the J-integral domains for threedimensional cases*

In three-dimensional problems the determination of node sets for the calculation of the *J*-integral is more complex than in two dimensions. As mentioned in section 3.3.1, the user has to define one node set for each node (or cluster of nodes) along the crack front in order from one end of to the other, including mid side nodes. Depending on the optional parameter NORMAL, the command for the *J*-integral calculation can have different forms. The definition of a curved crack front is only possible without using the NORMAL parameter.

Without NORMAL parameter:

```
**
** J-INTEGRAL DEFINITION OF A CURVED CRACK FRONT
** without NORMAL parameter
*CONTOUR INTEGRAL, CONTOURS=21, SYMM, OUTPUT=BOTH
 CTIP1, 1.0, 0.0, 0.0
 CTIP2, 1.0, 0.0, 0.5
 CTIP3, 1.0, 0.0, 1.0
 CTIP4, 0.5, 0.0, 1.0
 CTIP5, 0.0, 0.0, 1.0
**
```

Including the NORMAL parameter:

```
**
** J-INTEGRAL DEFINITION OF A STRAIGHT CRACK FRONT
** including the NORMAL parameter
**
*CONTOUR INTEGRAL, CONTOURS=21, SYMM, NORMAL, OUTPUT=BOTH
 1.0, 0.0, 0.0
CTIP1, CTIP2, CTIP3, CTIP4, CTIP5
**
```

If not just the crack tip nodes but planes are specified (as in Fig. 11 for the two-dimensional case), the user should care that the planes defined in the specific node sets are orthogonal to the crack front tangent, **t**, namely for curved crack fronts. The crack front tangent, **t**, is defined by the vector from the first node of one node set to the first node of the next set. A problem is that ABAQUS stores the node numbers of a set in an ascending order. If the smallest node numbers of two adjacent node sets are not at the same positions in their respective planes the crack front tangent is calculated incorrectly.

4.3 Results

The calculations have been performed using small and large deformations (parameter NLGEOM), respectively. The choice of the deformation theory influences the stresses and strains in the vicinity of the crack tip, but not the global behaviour. Therefore, the load vs loadline-displacement (V_{LL}) curve shown in Fig. 13 is identical for both calculations.

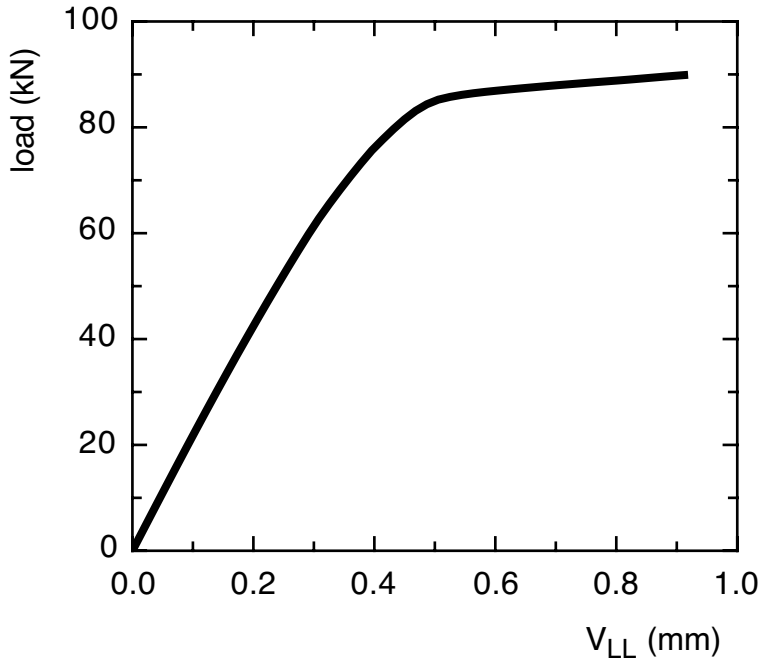

Figure 13: load vs loadline-displacement curve for the C(T) specimen; small or large deformation analyses yield identical curves.

The path dependence of the *J*-integral can be displayed in a J–V_{LL} curve, see Fig. 14 for a small deformation analysis and Fig. 15 for a large deformation analysis. The numbers J_02 to J_20 indicate the various contours or domains. Both figures also contain the *J*-integral evaluated according to ASTM standard 1737-96 [7] as a reference, which depends only on the load vs load-line displacement curve and hence is independent on the assumption of small or large deformations. As already stated in section 3.4, the path dependence of the *J*-integral is much more significant in a large deformation analysis. The far field value of *J* is reached with contour # 16 in the latter case, whereas in the small deformation analysis contour # 2 has already reached the far field value. Contour # 21 touches the boundary of the specimen, and the corresponding curves indicate that such a contour may not be used for *J*-integral evaluation.

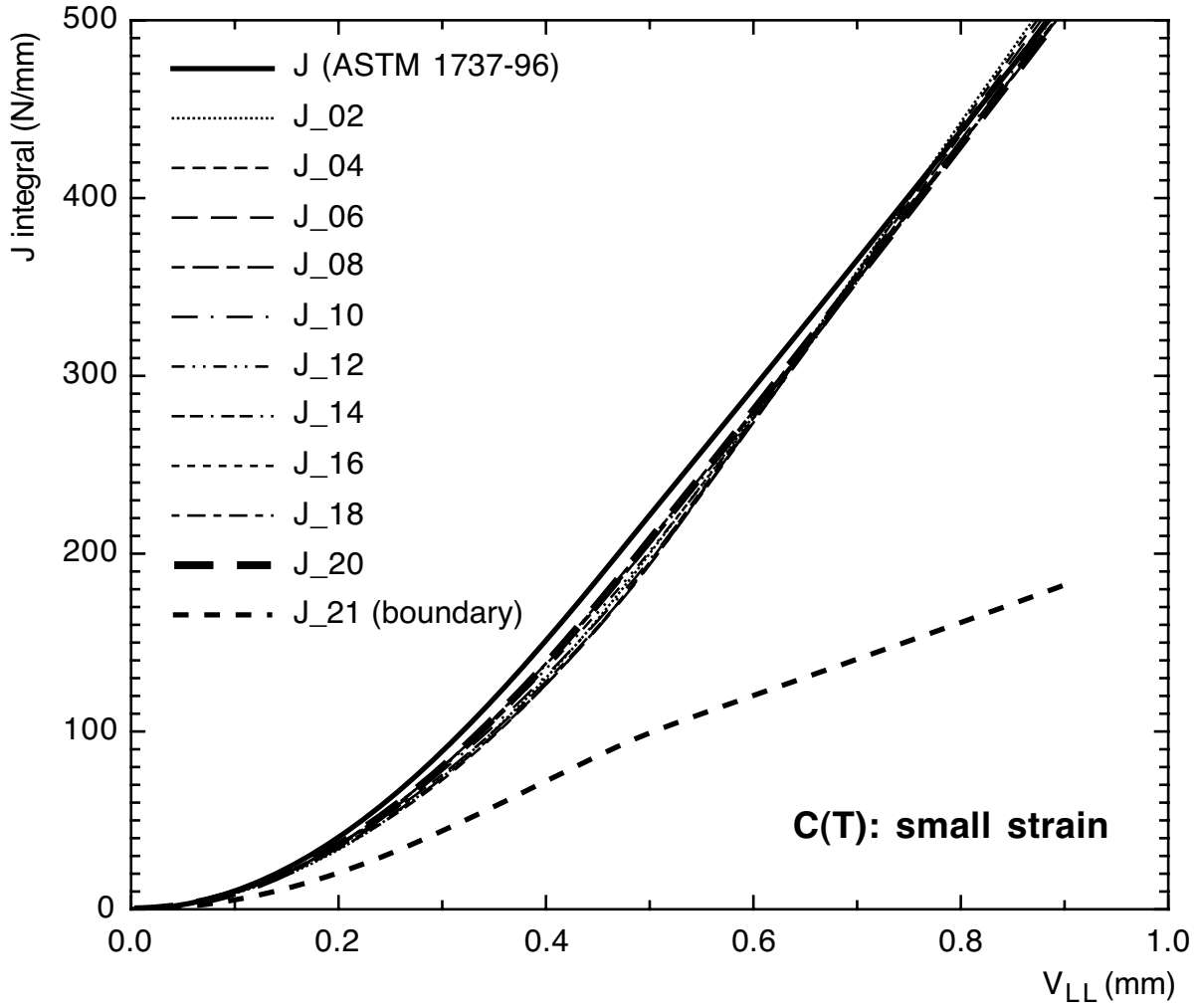

Figure 14: J–V_{LL} curve for the small deformation analysis

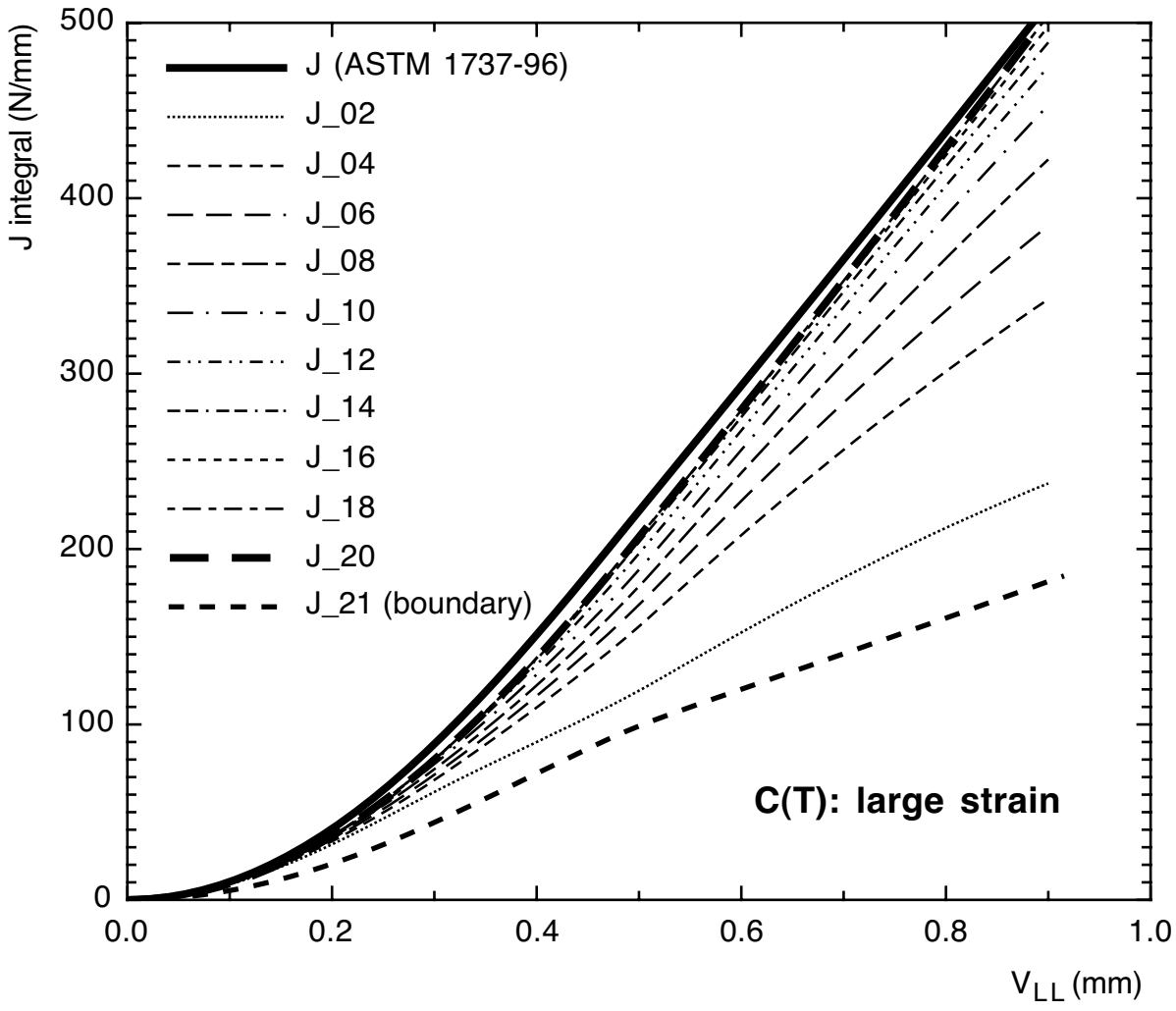

Figure 15: J–V_{LL} curve for large deformation analysis

As the work dissipated by plastic deformation always has to be positive, the calculated J values have to increase monotonically with the size of the domain - except contour # 21 touching the boundary - which is confirmed by Fig. 15. Any different result would indicate an error in the definition of contours or in the evaluation of J. Fig 16 illustrates the approach to a saturation value of J for two different load-line displacements. The highest J value calculated for any contour at a given loading ist the best approximation to the saturated far-field value.

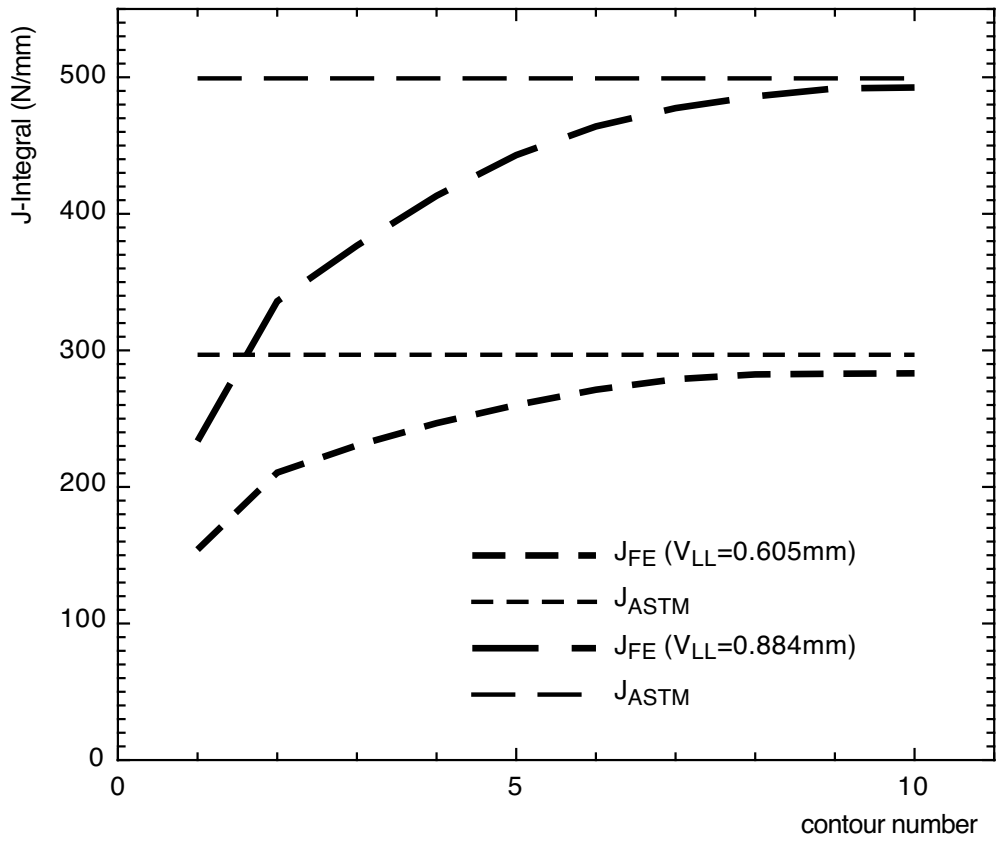

Figure 16: Path dependence of J in the large deformation analysis in comparison to the ASTM reference values.

Figure 17 finally compares the far field J values for large and small deformation analysis and the results of the ASTM standard formula based on the load vs load-line displacement curve. There is practically no difference between the small and large strain results if saturation values have been reached. In addition, the stress intensitiy factor K_I used in linear elastic fracture mechanics has been calculated according to ESIS P2-92 [40] and converted to J by eq. (10). Comparing this curve in Figure 16 with the elastic-plastic J-value, the limit up to which K_I is a valid fracture mechanics parameter can be examined. In the present example this limit is at a J value of about 60 N/mm, that is K=113 MPa$\sqrt{}$m. As the elastic-plastic J always has to be greater than the elastic one, the comparison between the two will also indicate any error made in the calculation of the former if it comes out to be less than the latter. In addition, the shape of the curves J vs V_{LL} is significant: J depends quadratically on V_{LL} in the elastic regime and linearly in the fully plastic regime.

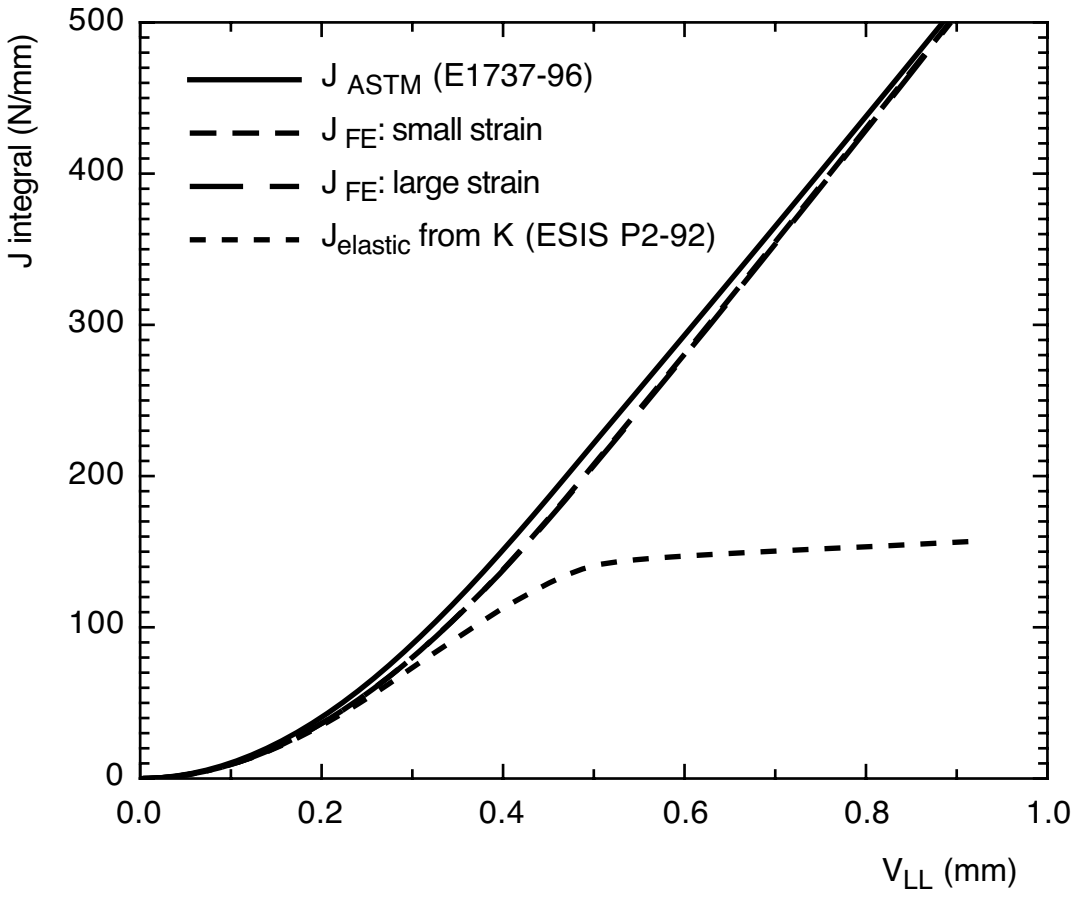

Figure 16: Far field *J*-integral (contour # 20) for small and large strain elastic-plastic analysis in comparison with ASTM evaluation and linear elastic *K*-analysis

5. Conclusions and Recommendations

- Comparably coarse meshes are sufficient; no special crack tip elements are required;
- Choose domain as large as possible but do not touch the boundary of the structure;
- Check if saturated value has been reached, otherwise increase the number of domains (contours);
- Do not average *J*-values calculated from various domains: the highest value is the best approximation to the real far-field *J*;
- A small-strain analysis will show less path dependence of *J* than a finite-strain analysis;
- No differences between small and large strain analyses exist with respect to *J* if saturated (far-field) values have been reached;
- Compare FE-results of contour (or domain) integral with formulas based on global load versus displacement data available for standard specimens ("experimental procedure");
- Compare FE-results of elastic-plastic contour integral with analytical *K*-formulas: the elastic-plastic *J* has to be grater than the purely elastic one;
- Check the shape of the curves *J* vs V_{LL}: *J* depends quadratically on V_{LL} in the elastic regime and linearly in the fully plastic regime.

6. References

[1] CHEREPANOV, C.P.: Crack propagation in continous media" Appl. Math. Mech. 31 (1967), 476-488.

[2] RICE, J.R.: A path independent integral and the approximate analysis of strain concentrations by notches and cracks, J. Appl. Mech. 35 (1968), 379-386.

[3] Wilson, W.K. and Osias, J.R.: "A comparison of finite element solutions for an elastic-plastic crack problem", Int. J. Fracture 14 (1978), R95.

[4] LARSSON, L.H.: "A calculational round robin in elastic-plastic fracture mechanics". Int. J. Press. Vess. and Piping 11 (1983), 207.

[5] LARSSON, L.H.: "EGF numerical round robin on EPFM". Proc. 3rd Int. Conf. on Numerical Methods in Fracture Mechanics (eds. A.R. LUXMOORE and D.R.J. OWEN), Swansea (UK), 1984.

[6] ESIS TC8: "Recommendations for use of FEM in fracture mechancis", ESIS Newsletter 15, 1991, 3-7.

[7] ASTM E 1737-96: "Standard test method for J-integral characterization of fracture toughness", Annual Book of ASTM Standards, Vol. 03.01.

[8] NOETHER, E.: "Invariante Variations-Probleme", Nachr. Gesell. Göttingen, Math.-Phys. Klasse 235 (1918).

[9] ESHELBY, J.D.: "The continuum theory of lattice defects", Prog. Solid States Physics 3 (1965), 79-114.

[10] GÜNTHER, W.: "Über einige Randintegrale der Elastomechanik" Abh. Brauchschw. Wiss. Ges. 14 (1962), 53-72.

[11] KNOWLES, J.K. and STERNBERG, E.: "On a class of conservation laws in linearized and finite elastostatics", Arch. Rat. Mech. Anal. 44 (1972), 187-211.

[12] BUDIANSKY, E. and RICE, J.R.: "Conservation laws and energy release rates", J. Appl. Mech. 40 (1973), 201-203.

[13] BUGGISCH, GROSS and KRÜGER, "Einige Erhaltungssätze der Kontinuumsmechanik vom J-Integral-Typ", Ing. Archiv 50 (1981), 103-111.

[14] KIENZLER, R.: "Konzepte der Bruchmechanik integrale Bruchkriterien", Grundlagen und Fortschritte der Ingenieurwissenschaften, Vieweg, Braunschweig, 1993.

[15] HUTCHINSON, J.W.: "Singular behaviour at the end of a tensile crack in a hardening material" J. Mech. Phys. Solids 16 (1968), 13-31.

[16] RICE, J.R., and ROSENGREN, G.F.: "Plane strain deformation near a crack-tip in a power-law hardening material", J. Mech. Phys. Solids 16 (1968), 1-12.

[17] ABAQUS/Standard Version 6.1, User's Manual Vol. I, 7.8.2, 2000.

[18] PARKS, D.M.: "The virtual crack extension method for nonlinear material behavior", Computer Methods in Applied Mechanics and Engineering 12 (1977), 353-364.

[19] PARKS, D.M.: "Virtual crack extension - A general finite element technique for J-integral evaluation", Proc. 1st Int. Conf Numerical Methods in Fracture Mechanics, Swansea (UK), 1978, 464-478.

[20] DELORENZI, H.G.: "On the energy release rate and the J-integral for 3D crack configurations", J. Fracture 19 (1982), 183-193.

[21] KORDISCH, H.: "Untersuchungen zum Verhalten von Rissen unter überlagerter Normal- und Scherbeanspruchung", Dissertation, Karlsruhe, 1982.

[22] KIKUCHI, M., MIYAMOTO, H., and SAKAGUCHI, Y.: "Evaluation of three-dimensional J-integral of semi-elliptical surface crack in pressure vessel", Trans.5th Int. Conf. Structural Mechanics in Reactor Technology (5th SMiRT), paper G7/2, Berlin, 1979.

[23] AMESTOY, M., BUI, H.D., and LABBENS, R.: "On the definition of local path independent integrals in 3D crack problems", Mech. Res. Communications (1981).

[24] BAKKER, A.: "The three-dimensional *J*-Integral", Delft University of Technology (The Netherlands), Report WTHD 167, 1984.

[25] DELORENZI, H.G.: "Energy release rate calculations by the finite element method", General Electric Technical Infomation Series, Report No. 82CRD205, 1982.

[26] SIEGELE, D.: "3D crack propagation using ADINA", Computers & Structures 32 (1989), 639-645.

[27] MUSCATI, A. and LEE, D.J.: "Elastic-plastic finite element analysis of thermally loaded cracked structures", Int. J. Fracture 25 (1984), 2276-246.

[28] KIKUCHI, M. and MIYAMOTO, H.: "Evaluation of J_k integrals for a crack in multiphase materials", Recent Research on Mechanical Behavior of Materials, Bulletin of Fracture Mechanics Laboratory, Vol. 1, Science University of Tokyo, 1982.

[29] ATLURI, S.N., NISHIOKA, T. and NAKAGAKI, M.: "Incremental path-independent integrals in inelastic and dynamic fracture mechanics", Engineering Fracture Mechanics 20 (1984), 209-244.

[30] BRUST, F. W., NISHIOKA, T. and ATLURI, S. N.: "Further studies on elastic-plastic stable fracture utilizing the T^*-Integral". Engineering Fracture Mechanics 22 (1985), 1079-1103.

[31] YUAN, H. and BROCKS, W.: "Numerical investigations on the significance of *J* for large stable crack growth", Engineering Fracture Mechanics 32 (1989), 459-468.

[32] YUAN, H.: "Untersuchung bruchmechanischer Parameter für elastisch-plastisches Rißwachstum", Fortschr.-Ber. VDI Reihe 18 Nr. 82, Düsseldorf: VDI-Verlag, 1990.

[33] YUAN, H. and BROCKS, W.: On the *J*-integral concept for elastic-plastic crack extension, Nuclear Engineering and Design 131 (1991), 157-173.

[34] RICE, J.R.: "An examination of the fracture mechanics energy balance from the point of view of continuum mechanics", Proc. 1st Int. Conf. on Fracture (eds. T. YOKOBORI, T. KAWASAKI and J.K. SWEDLOW), Sendai (Japan), 1965, 309-340.

[35] RICE, J.R.: "The mechanics of quasi-static crack growth", Proc. 8th Int. Congress of Applied Mechanics (ed. R.E. KELLY), 1979, 191-216.

[36] BARSOUM, R.S.: "Triangular quarterpoint elements as elastic and perfectly-plastic crack tip elements", Int. J. Num. Meth. Engng. 11 (1977), 85-98.

[37] BROCKS, W.: "Zur numerischen Ermittlung des Spannungsintensitätsfaktors in der linear elastischen Bruchmechanik", Strukturmechanik und numerische Verfahren (Hrsg. R. Diekkämper, H.-J. Niemann), Köln-Braunsfeld: R. Müller (1982), 88-101.

[38] BROCKS, W. and OLSCHEWSKI, J.: On *J*-dominance of crack-tip fields in largely yielded 3D structures", Int. J. Solids Structures 22 (1986), 693-708.

[39] BROCKS, W., MÜLLER, W. and OLSCHEWSKI, J.: Experiences in applying ADINA to the analysis of crack tip fields in elastic-plastic fracture mechanics", Nonlinear Finite Element Analysis and ADINA, Computers and Structures 21 (1985), No. 1/2, 137-158.

[40] ESIS P2-92: “ESIS recommendations for determining the fracture resistance of ductile materials.”, European Structural Integrity Society (1992)